JOURNAL OF CATALYSIS 4, 140–152 (1965)

The Recombination of Atoms on Pd–Au Alloys

P. G. DICKENS, J. W. LINNETT, AND W. PALCZEWSKA

From the Inorganic Chemistry Laboratory, Oxford University, Oxford, England

Received April 7, 1964; revised July 24, 1964

Atom recombination efficiencies have been measured for hydrogen and oxygen on a series of annealed Pd–Au foils. With hydrogen, the recombination coefficient, γ, was found to be dependent on the time of exposure of the foil to the atomic flux. For a "hydrogen-free" condition (short exposure time) a maximum activity was found in the composition range 0–55% Au ($\gamma \sim 10^{-2}$). A decrease in activity was found in passing from 55% to 100% Au ($\gamma \sim 10^{-3}$ for pure Au). For a "hydrogen-saturated" condition (long exposure time), the variation in γ on passing from pure Pd to pure Au was greatly reduced, though the value of γ for pure Au remained the same. With oxygen the recombination coefficients were very low ($\gamma \sim 10^{-3}$ to 10^{-4}) and showed no systematic variation with alloy composition. In all the recombinations studied the disappearance of atoms from the gas phase was found to be first order. The mechanistic consequences of this are discussed.

The high catalytic efficiencies of transition metals for hydrogenation reactions are often attributed to the presence of unfilled *d* bands in such metals. The binary alloy systems formed by the Group IB metals Au, Ag, and Cu, with Group VIII metals Pd, Pt, or Ni, are suitable materials for the demonstration of the role of *d*-band vacancies in catalytic processes. An increasing proportion of IB metal in the solid solution causes the *d* band of the alloy to become progressively filled (by donation of *s* electrons), as is shown by magnetic susceptibility changes. At a composition in the region of ~60% of the IB metal the *d* band becomes completely filled and the alloy diamagnetic (*1*). A change in catalytic efficiency for hydrogenation reactions might be expected at this point. Such an effect was demonstrated by Couper and Eley (*2*) for the parahydrogen conversion on Pd–Au alloys. Similar effects in hydrogen equilibration reactions have been found for the systems Pt–Cu (*3*), Cu–Ni (*4*) and Pd–Cu (*4*), but differences in detailed behavior are found and these have been discussed by Bond (*5*).

The purpose of the present work was to test these ideas by measuring the catalytic efficiencies of a series of Pd–Au foils for atom recombination. Rates of both hydrogen and oxygen atom recombinations at room temperature have been measured. In principle, atom recombinations on such alloys provide the simplest systems available for the study of electronic factors in catalysis.

EXPERIMENTAL DETAILS

Method

The side arm technique of Smith (*6*) was employed. The principle of the method can be stated briefly. A constant source of atoms is produced at one end of a long cylindrical tube constituting a closed sidearm. The walls of a section of the cylindrical tube are lined with the catalytic material. Under the low pressure conditions maintained in the sidearm, atoms decay along the tube to give a steady state distribution in which the rates of diffusion and wall removal are balanced. The rate of change of atom concentration along the axis of the tube (within the catalyst region) is a measure of the rate of atom recombination at that surface. Quantitatively, the recombination coefficient, γ, defined as the fraction of atomic collisions with the walls leading to recombination, is determined.

For an infinite cylinder of uniform catalytic activity the axial decay of atom concentration, n, with distance from the source, x, is given by

$$n \sim n_0 \exp\left[-(\gamma\bar{c}/2RD)^{1/2}x\right]$$

where n_0 is the atom concentration at $x = 0$, $\bar{c}$ is the mean atomic speed, R is the tube radius, and D is the binary diffusion coefficient for the mixture. This equation is a good approximation to the exact theoretical expression for this model (*7*) and can be used for the calculation of γ under conditions of low atom concentration ($<10\%$) and for values of $4D/c\gamma R > 10$. In ref. *7* the effect of a catalytic probe, as used in the measurement of atom concentration, on the axial atomic concentration gradient was also investigated. It was shown that it is only necessary to make probe measurements sufficiently far down the tube from the atom source ($>10R$) for the *gradient* of the log n vs x plot to be characteristic of the wall surface alone and to be independent of the probe activity. Schofield (*8*) has investigated the theoretical axial concentration gradient for a model in which the surface activity of the tube undergoes a discontinuous change at a distance down the tube X_1 (as is realized by the insertion of a sleeve of greater catalytic activity into the sidearm). He found that the concentration gradient characteristic of the *sleeve* material extends from $x > X_1$ right up to the boundary at X_1. In the present work measurements were made for values of x in the range $10R < X_1 < x$, and hence the use of the above equation is justifiable.

Apparatus

The apparatus and its layout were essentially those used by Linnett and Greaves (*9*). A somewhat larger sidearm was used (3 cm in diameter, 200 cm long) to ensure that hydrodynamic conditions prevailed ($2R > 10\lambda$, where $2R$ is the diameter of the tube and λ is the mean free path in the gas). Atoms were produced in an air-cooled silica discharge tube surrounded by a coil of six turns of 6-mm diameter copper tubing. The coil was activated by the output from a RCA high frequency communications transmitter, operating at a fixed frequency of 15 Mc/sec. The Pd–Au foils were made into cylinders 10 cm long and ~3 cm in diameter, which fitted snugly inside the water-jacketed pyrex sidearm. The relative atom concentration along the axis of the sidearm was measured by the temperature rise of a mobile silver-coated thermocouple probe. A fixed monitor probe of the same type was positioned in a small sidearm at right angles to the main one 15 cm down stream from the discharge tube. The monitor probe provided a necessary check on the constancy of the atom concentration at the source, and allowed all mobile probe readings to be "normalized" by division by the monitor probe reading. The sleeve of foil was positioned 30 cm downstream from the discharge tube, well clear of the luminous plasma. The ambient pressure in the sidearm (~250 μ) was measured with a McLeod gauge positioned 150 cm downstream from the discharge tube.

Materials

Pd–Au alloys containing 0, 12, 31, 45, 72, 100 atomic % Au, in the form of foils 2/1000-inch thick, were supplied by Mond Nickel Co. Before use the foils were first cleaned chemically. Usually the foils were then annealed by heating in a vacuum furnace at 700–900°C for about an hour, and then gradually cooled *in vacuo* over a period of 4–5 hr. A few measurements were made on unannealed foils. Pure oxygen and hydrogen were prepared by electrolysis (and impurities of each in the other were removed by passage through heated platinized asbestos). The gases were saturated with water vapor at 26°C before passing into the discharge tube via a permanent leak.

Because the gas is wet, it will contain, in the tube beyond the discharge, a small proportion of OH radicals. These will react with H_2 according to $OH + H_2 = H_2O + H$. For this reaction Kaufmann and Del Greco (*10*) give $k = 1.5 \times 10^9$ liter per mole/sec. At a pressure of 250 μ therefore

$$d[\mathrm{H}]/dt = -d[\mathrm{OH}]/dt = k'[\mathrm{OH}]$$

where $k' = 2 \times 10^4$ sec^{-1}. When hydrogen atoms are being removed by recombination at the wall of the 3-cm tube

$$-(1/[\mathrm{H}])(d[\mathrm{H}]/dt) \sim 10^5\gamma.$$

When $\gamma = 10^{-4}$, log [H] falls by 0.2 in 1 cm (see result depicted in Fig. 1). Because of the greater first order velocity constant for the conversion of OH into H ($k' = 2 \times 10^4$ sec^{-1}), the drop in log [OH] will be fourfold greater, and, because of the lower diffusion coefficient of OH, it will be increased by a further factor of 3. Consequently the OH radical concentration will fall to one-hundredth of its value in 1 cm, the radicals being converted to hydrogen atoms. Therefore, it is possible to be confident that all the hydroxyl radicals will have been converted to hydrogen atoms in the region near the discharge and the early part of the sidearm, and that there will be none in the test region. This is the case because the test location is 15 cm down the sidearm, which itself starts 15 cm downstream from the discharge. The hydrogen atoms persist into this region because of the low activity of the Pyrex glass from which the apparatus is constructed.

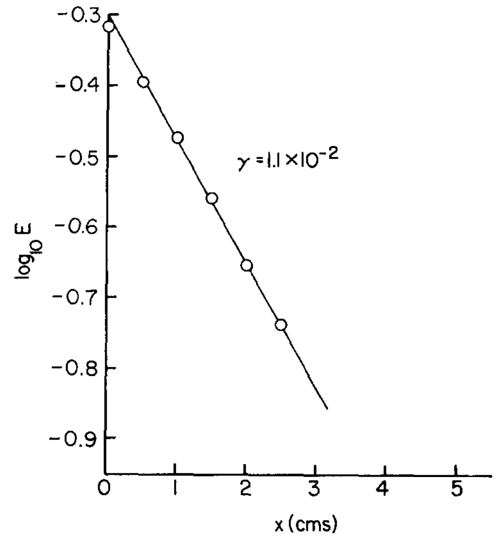

FIG. 1. Plot of $\log_{10} E$ versus x for hydrogen atom recombination; foil III (31% Au), exposure time 2–4 hr, annealing temperature 750°C.

Procedure

Preliminary experiments revealed characteristic differences in the behavior of the alloys towards hydrogen and oxygen atoms, respectively. Different procedures of measurement were adopted in the two cases.

(i) Hydrogen Atom Recombination

Pd and Pd-rich alloys absorbed hydrogen and their catalytic efficiencies for hydrogen atom recombination were found to decrease with time of exposure to the atomized gas. It was therefore attempted to measure the change in catalytic efficiency with time and obtain recombination coefficients characteristic of both the hydrogen-free and hydrogen-saturated alloys. After switching on the discharge, it was necessary to allow the apparatus about 1 hr, sometimes as much as 3 hr, in which to settle down before reproducible results could be obtained. Thermocouple probe readings were taken at 1 or ½ cm intervals along the axis of the cylinder of foil, moving the probe first downstream and then back again to recover the first two points. Plots of

$$\log_{10} \frac{\text{mobile probe emf}}{\text{monitor probe emf}} \ (E)$$

versus distance (x) were then made; γ was calculated from the relation

$$\gamma = \beta^2 2RD/\bar{c},$$

where

$$\beta = d(\ln E)/dx$$

$2R$ is the diameter of the foil cylinder, D is the diffusion coefficient for H–H$_2$ mixtures (*11*) and $\bar{c}$ is the mean speed of H atoms at the experimental temperature. A single measurement of β took about 15 min to accomplish. A mean value of γ over a period 1–2 hr was obtained from several measurements of β in this time interval, and this was quoted as the value of γ characteristic of the exposure time up to that particular interval. Subsequent plots were made over periods of up to 45 hr. The catalytic efficiency was found to fall slowly before coming to a final value taken to be that characteristic of the hydrogen-saturated alloy. The change in efficiency over the time interval required to obtain a single mean value of γ was usually small. It was found that the annealing temperature of the foils had a significant effect on their subsequent catalytic efficiency. The efficiencies of unannealed foils were variable and at least an order of magnitude higher than of foils annealed at 700°C. Consequently a uniform annealing pretreatment (1 hr at 700–750°C) was adopted for all the foils. It was also found that the hydrogen poisoning effect was accelerated, considerably in certain cases, by subsequent desorption and annealing *in vacuo* at somewhat higher temperatures (about 900°C). This treatment did not significantly affect the initial catalytic efficiency, assumed to be that of the alloy in the hydrogen-free condition, but did cause a more rapid falling off of efficiency with time of exposure to hydrogen atoms. The same foil, or in most cases a second foil of the same alloy, was thus annealed *in vacuo* at 900°C for $\frac{1}{2}$–$1\frac{1}{2}$ hr, and this foil was used to obtain values of γ after a long exposure time corresponding to the hydrogen-saturated condition. At intermediate exposure times it was found that the plots of $\log_{10} E$ versus distance often consisted of two linear portions of different slopes. The first portion, corresponding to the first few centimeters of foil closest to the discharge tube (and therefore exposed to the highest concentration of H atoms), had a noticeably lower slope corresponding to a lower recombination efficiency. The second section of the foil was more reactive, being less saturated with hydrogen. The slopes of both portions decreased slowly with time, converging towards the same constant value as the whole foil gradually became saturated. Further procedural details in individual cases are summarized in the Results Section. Attempts to analyze the saturated alloys for hydrogen content were unsuccessful. Preliminary analyses with foils of Pd and 72% Au alloy, following long exposures to H atoms, were carried out by A.E.R.E. Harwell. These revealed values of 2500 and 20 ppm hydrogen, respectively. Unfortunately the delay in having the analyses done (several weeks) nearly certainly made these figures valueless since it was subsequently discovered that it is known (*13*) that hydrogen is lost from Pd–Au alloys within a few days of exposure to the atmosphere.

(*ii*) *Oxygen Atom Recombination*

The procedure adopted here was quite straightforward since the activities of the alloys showed no systematic changes with time of exposure to oxygen atoms. Measurements were made on both unannealed and annealed samples. Straight line plots of $\log_{10} E$ vs x were invariably found, though the actual values of γ were less reproducible than had been found with similar measurements on evaporated metal films. The value of the diffusion coefficient given by Andrussov (*12*) was used in the calculation of γ.

EXPERIMENTAL RESULTS

Hydrogen Atom Recombination

The complete set of results and relevant comments are shown in Table 1. An extended commentary on the results for one of the alloys (Au 31%–Pd 69%) is included here in order to illustrate the complex behavior typically encountered in this series of measurements and in order to explain in more detail the procedure summarized in Table 1. A foil labeled II was annealed *in vacuo* at 700–750°C for 1 hr and allowed to cool gradually. The first reproducible measurements were made in the period of 2–3 hr after switching on the discharge. The initial value of $\gamma = 1.1 - 1.2 \times 10^{-2}$ remained unchanged over some 30 hr of exposure of the foil; that is, the alloy in this condition appeared to be resistant to hydrogen poisoning. The foil was then reannealed *in vacuo* at 900°C for $\frac{1}{2}$ hr. The initial value of γ after 1–2 hr exposure was unchanged at 1.1×10^{-2}; this value was taken to be characteristic of the hydrogen-free alloy. Over the next 26 hr of exposure to hydrogen atoms, the value of γ fell to 7.2×10^{-3} and the foil developed a deformed appearance. The foil was then given a second annealing *in vacuo* at 900°C this time for 1 hr. After 5–6 hr of further exposure to hydrogen atoms the first centimeter of the foil appeared to have a much lower value of γ, 1.2×10^{-3}, characteristic of the more saturated alloy. This value was unreliable, however (marked ? in Table 1) since the slope β was determined

TABLE 1
RECOMBINATION COEFFICIENTS γ FOR HYDROGEN ATOMS[a]

Alloy	No. of sample	Annealing conditions	T (°C)	p (μ)	$2R$ (cm)	$\beta/\ln 10$	Time of exposure (hours)	γ	Remarks
Au	I	700°C 1½ hr	23.0	239	2.80	−0.041	5–8	5.7×10^{-4}	No change with exposure time
			26.0	228			14–17	5.8×10^{-4}	
Au 12% Pd 88%	II	700–750°C 1 hr	21	218.5	2.85	−0.16	3–4	9.5×10^{-3}	
				222.5		−0.15	5–6	8.23×10^{-3}	
			20	218		−0.098	12½–14½	$\mathit{3.60} \times \mathit{10}^{-3}$	First 2 cm
						−0.12	—	5.70×10^{-3}	
			22	212		−0.10	16½–17½	$\mathit{4.0} \times \mathit{10}^{-3}$	About 2 cm of foil swollen
			22	218		−0.081	20–22	$\mathit{2.5} \times \mathit{10}^{-3}$	First 2.5 cm
	III	900°C 1½ hr	23	249	2.85	−0.071	3½–4½	$\mathit{?1.6} \times \mathit{10}^{-3}$	First 1.5 cm
						−0.14		5.9×10^{-3}	
			23	250		−0.071	8–9½	$\mathit{?2.5} \times \mathit{10}^{-3}$	2 points only
						−0.14		6.2×10^{-3}	
				240		−0.070	16½–17½	$\mathit{?1.5} \times \mathit{10}^{-3}$	2 points only
						−0.13		5.2×10^{-3}	
				249		−0.075	21–22½	$\mathit{?1.7} \times \mathit{10}^{-3}$	2 points only
						0.14		6.3×10^{-3}	
Au 31% Pd 69%	II	700–750°C 1 hr	23	224.5	2.80	−0.18	2–3½	1.1×10^{-2}	No marked change in the appearance of the foil
				224		−0.18	6–7	1.1×10^{-2}	
				227		−0.19	9–11	1.2×10^{-2}	
				226		−0.18	12½–15½	1.2×10^{-2}	
				226.5		−0.18	19–21½	1.2×10^{-2}	
				227		−0.18	22½–24½	1.2×10^{-2}	
				227		−0.18	32–33	1.2×10^{-2}	
	II	900°C ½ hr	21.5	219	2.80	−0.17	1–2	1.1×10^{-2}	Foil became swollen and deformed
			21.5	221		−0.15	6½–8	8.6×10^{-3}	
			21–5	218		−0.14	15–18	7.5×10^{-3}	
			20	220		−0.14	25–28	7.2×10^{-3}	
			21	216.5		−0.088	36–38	$\mathit{?2.9} \times \mathit{10}^{-3}$	First 1 cm only
						−0.14		7.3×10^{-3}	
	II	900°C 1 hr	23	252	2.80	−0.06	5–6	$\mathit{?1.2} \times \mathit{10}^{-3}$	First 1 cm only
						−0.19		1.2×10^{-2}	
						−0.075	9–10	$\mathit{?1.8} \times \mathit{10}^{-3}$	First 1.5 cm only
						−0.17		9.6×10^{-3}	
	III	700–759°C 1 hr	23	222.5	2.75	−0.17	2–4	1.1×10^{-2}	
				221		−0.18	8–9	1.2×10^{-2}	
Au 31% Pd 69%	III	900°C 1½ hr	22	241.5	2.80	−0.11	5–7½	$\mathit{4.1} \times \mathit{10}^{-3}$	First 2.5 cm
						−0.15		7.7×10^{-3}	
				242		−0.078	10½–11½	$\mathit{2.0} \times \mathit{10}^{-3}$	First 2.5 cm
						−0.13		5.9×10^{-3}	
				245		−0.062	16–18	$\mathit{1.3} \times \mathit{10}^{-3}$	First 2.5 cm
						−0.11		4.1×10^{-3}	
				242–5		−0.071	22½–23½	$\mathit{1.7} \times \mathit{10}^{-3}$	First 2.5 cm
						−0.12		4.6×10^{-3}	The foil was deformed but not swollen

TABLE 1 (*Continued*)

Alloy	No. of sample	Annealing conditions	T (°C)	p (μ)	$2R$ (cm)	$\beta/\ln 10$	Time of exposure (hours)	γ	Remarks
Au 45% Pd 55%	III	750°C 1 hr	23.0	219.5	2.85	−0.16	3–4	1.0×10^{-2}	Surface of the foil apparently unchanged, but the alloy became more flexible
				224.5		−0.14	5–6½	7.2×10^{-3}	
				222		−0.16	9–10	9.1×10^{-3}	
				225		−0.14	22–24½	7.6×10^{-3}	
	II	700°C, 1 hr		228.5	2.85	−0.16	6–7	9.3×10^{-3}	
		900°C, 1 hr	26.0	230		−0.073	14–18	1.2×10^{-3}	
		(700°C, 1 hr)		226		−0.075	22–25	2.1×10^{-3}	
Au 72% Pd 28%	III	750°C, 1 hr	20.0	225	2.85	−0.12	3–4	5.5×10^{-3}	No distinct change in the appearance of the foil
			21.0	223		−0.11	8–9	4.8×10^{-3}	
				224		−0.11	9–10½	4.5×10^{-3}	
			22.0	223.5		−0.10	15½–18	3.8×10^{-3}	
	II	700°C, 1 hr	26.0	230	2.85	−0.11	8–10	4.7×10^{-3}	
		900°C, 1 hr		235		−0.082	18–20½	2.4×10^{-3}	
		700°C, 1 hr		230		−0.068	29½–33½	1.7×10^{-3}	
				233		−0.065	39½–44	1.5×10^{-3}	
Pd	II	Not annealed	24	223.5	2.95	−0.16	4–7	1.0×10^{-2}	Foil swollen
		Not annealed	24.5	225.5	(2.95)	−0.15	13½–16½	9.2×10^{-3}	Change of shape
		700–750°C 1 hr	26	233.5	2.80	−0.15	10–13	8.5×10^{-3}	Change of shape
				235.0	2.75	−0.16	22–24½	9.0×10^{-3}	
				236.0	2.70	−0.16	33½–35½	8.6×10^{-3}	Change of shape
		700°C, 2 hr	21	255.0	2.85	−0.062	27–30	$\mathit{1.3} \times \mathit{10}^{-3}$	First 3.5 cm
				255.0	2.85	−0.089		2.6×10^{-3}	
		900°C, ½ hr		250	2.85	—0.061	32–34	1.2×10^{-3}	First 3 cm
	I	850°C, 1 hr	21	247	2.80	−0.063	5–7	$\mathit{1.3} \times \mathit{10}^{-3}$	First 2 cm
		900°C, ½ hr		247	2.80	—0.086		2.4×10^{-3}	
				241	2.80	−0.061	8–10	$\mathit{1.2} \times \mathit{10}^{-3}$	First 2 cm
				241	2.80	−0.093 (?)		2.9×10^{-3}	First 2–3 cm more swollen than the remainder

[a] T = sidearm temperature; p = gas pressure; $\beta = d(\ln E)/dx$; R = radius of cylinder.

from only two points. These data are summarized in the table (*? 1.2* $\times$ *10^{-3}*, 1.2×10^{-2}, 1 cm). The italicized value refers to the first part of the foil, the second value to the remainder. A second foil (III) was annealed *in vacuo* at 700–750°C for 1 hr and the initial value of $\gamma = 1.1 \times 10^{-2}$ was identical with that for foil II. Experimental points are shown in Fig. 1. This value is recorded in Fig. 4 as characteristic of this composition of alloy in the hydrogen-free condition. Finally foil (III) was annealed *in vacuo* at 900°C for 1 hr. After 5–7 hr the log E vs x plot developed two linear portions, as shown in Fig. 2. The value for γ over the first part had dropped to 4.1×10^{-3} and over the remainder to 7.7×10^{-3}. After 23 hr exposure the relative values were 1.7×10^{-3} and 4.6×10^{-3} (Fig. 3). The foil had developed a deformed appearance but was not swollen. The value of $\gamma = 1.7 \times 10^{-3}$ was taken as the value characteristic of the saturated alloy and is plotted accordingly in Fig. 4.

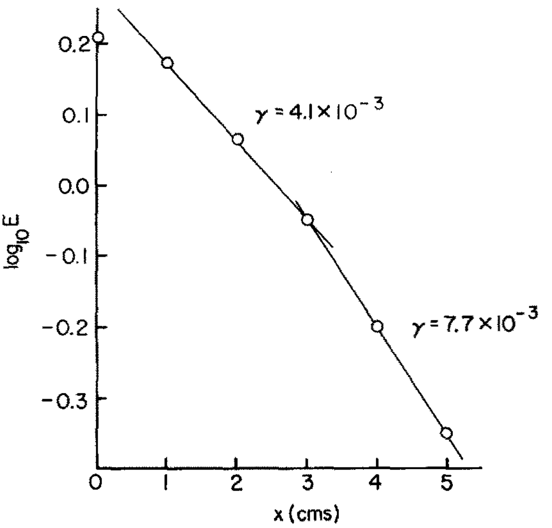

FIG. 2. Plot of $\log_{10} E$ versus x for hydrogen atom recombination; foil III (31% Au), exposure time 5–7½ hr, annealing temperature 900°C.

In Fig. 4 are plotted values of $\log_{10} \gamma$ vs alloy composition, for both the hydrogen-free condition (marked ○) and for the hydrogen-saturated condition (marked ●). The hydrogen-free value for Pd is probably too low since in this case the first measurement made on foil II, after annealing for 1 hr *in vacuo* at 700–750°C, was made after 10 hr exposure to hydrogen atoms. The true value is unlikely to be higher than 1×10^{-2}, though, since this is the value found for the *unannealed* sample after a short exposure time (4 hr).

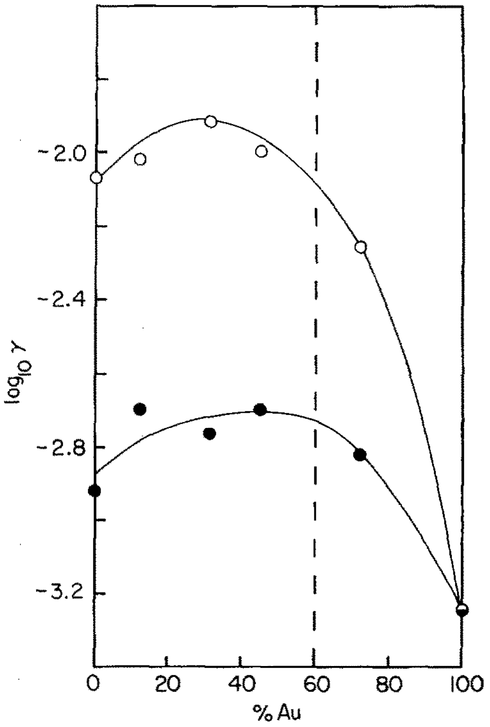

FIG. 4. Variation of $\log_{10} \gamma$ for hydrogen atom recombination with Pd–Au alloy composition: ○, hydrogen-free condition; ●, hydrogen-saturated condition.

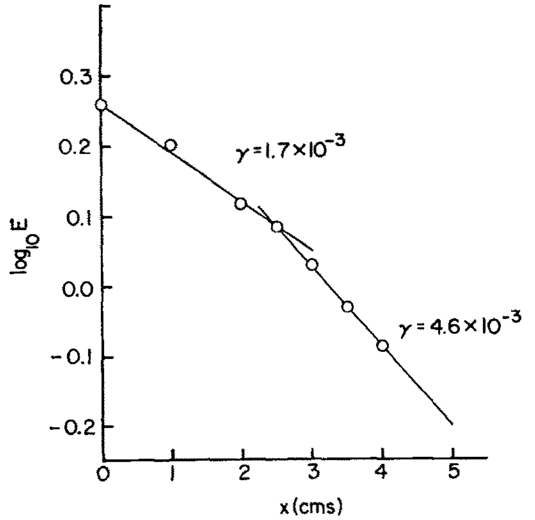

FIG. 3. Plot of $\log_{10} E$ versus x, for hydrogen atom recombination; foil III (31% Au), exposure time 22½–23½ hours, annealing temperature 900°C.

Oxygen Atom Recombination

Measurements were made on some or all of the alloys after each of three different annealing treatments: (a) not annealed; measurements were made for the pure metals only; (b) annealed by heating for 1 hr *in vacuo* at 700–750°C, followed by gradual cooling, measurements were made on all the alloys and the pure metals; (c) annealed by heating *in vacuo* for one or more hours at 700°C followed by a shorter period of ½–1 hr at 900°C, followed by gradual cooling, measurements were made on the pure metals and on two of the alloys.

The results are shown in Table 2.

TABLE 2

RECOMBINATION COEFFICIENTS γ FOR OXYGEN ATOMS[a]

Composition	Pd		88% Pd	69% Pd	55% Pd	28% Pd	Au		
No. of sample	I	II	I	I	I	I	I	II	III
Foils not annealed	1.3×10^{-2} 1.0×10^{-2} 1.3×10^{-2} 1.3×10^{-2} 1.4×10^{-2}	—	—	—	—	—	1.3×10^{-2} 1.7×10^{-2} 1.8×10^{-2} 2.2×10^{-2} 2.7×10^{-2}	1.3×10^{-2} 1.6×10^{-2}	—
Foil annealed by heating for 1 hr *in vacuo* at 700–750°C, followed by gradual cooling	4.5×10^{-4} 8.7×10^{-4} 8.3×10^{-4} 6.9×10^{-4}	3.9×10^{-3} 4.4×10^{-3}	3.7×10^{-4} 3.6×10^{-4} 6.8×10^{-4} 2.7×10^{-4}	4.0×10^{-3} 3.9×10^{-4} 5.6×10^{-4} 3.3×10^{-4}	2.0×10^{-3}	1.6×10^{-3}	7.3×10^{-4} 8.7×10^{-4}	2.8×10^{-3}	2.4×10^{-3} 2.4×10^{-3}
Foils annealed by heating for 1 hr *in vacuo* at 700°C, followed by $\frac{1}{2}$–1 hr at 900°C, followed by gradual cooling	—	8.8×10^{-4} 3.0×10^{-4} 6.1×10^{-4} 3.3×10^{-4}	—	—	2.9×10^{-4} 3.0×10^{-4}	3.8×10^{-4} 3.0×10^{-4}	2.8×10^{-4}	3.9×10^{-4} 3.9×10^{-4} 4.0×10^{-4}	—

[a] Successive values of γ after treatment.

Discussion

Hydrogen Atom Recombination

The main empirical conclusions to be drawn from the results are:

(a) Within the limits of accuracy of the measurements (probable error in $\gamma \sim 10\%$), the recombination process was first order in hydrogen atom concentration for all the alloys.

(b) For the hydrogen-free alloys the highest catalytic activity was found for compositions between 100% and 55% Pd. A somewhat lower value of γ was found for a composition of 72% Au and a considerably lower value still was found for pure Au; γ fell by a factor of ~15 on passing from pure Pd to pure Au.

(c) For the hydrogen-saturated alloys, lower values of γ were found for Pd-containing alloys but the value for pure Au was unchanged. The dependence of γ on composition was less marked; the fall in γ passing from Pd to Au was only twofold.

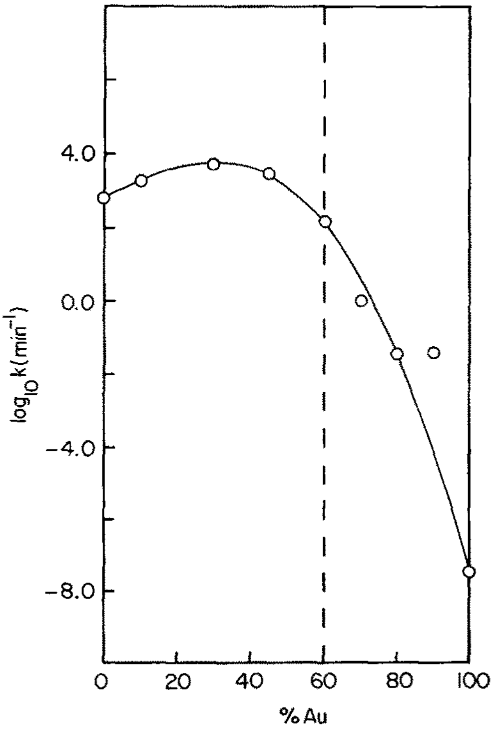

FIG. 5. Variation of activity for parahydrogen conversion with Pd–Au alloy composition.

An apparent maximum was found in the $\log_{10} \gamma$ vs composition plot (Fig. 4), for the hydrogen-free alloys, in the region of 30% Au. A similar maximum in *activity* (not activation energy) was found by Eley and Couper (*2*) for the para-H_2 conversion. A plot of their results as quoted by Bond (*5*) is included (Fig. 5) to illustrate the close similarity between the activity patterns for para-H_2 conversion and H atom recombination on Pd–Au alloys. A poisoning effect following exposure of Pd–Au alloys to H atoms was also reported by Eley and Couper (*2*). These authors found that the activation energy for the para-H_2 conversion on Pd wire, saturated with hydrogen by exposure to hydrogen atoms, was ~11 kcal/mole as compared with a value of ~4 kcal/mole for hydrogen-free Pd. That is, the activation energy was increased to a value somewhat larger than that found for the hydrogen-free 60% Au alloy but less than that for pure Au (17 kcal/mole).

The acceleration of the poisoning effect, following desorption *in vacuo* at 900°C, found in the present work, can be attributed to the "opening" of pores and rifts in the metal leading to a more rapid subsequent sorption (*13*).

The only previous study of hydrogen atom recombination on Pd–Au alloys is that recently published by Wood and Wise (*14*). These authors used the alloys in the form of wires and employed a filament probe technique. The actual alloy under study constituted the filament of the probe and the atom concentration at the probe was estimated by the change in power input necessary to maintain its temperature (i.e., resistance) constant. Since the resistances of such wires change with the amount of dissolved hydrogen, this technique necessitated working with the wires in a consistently saturated condition. That is, derived values of γ refer to a hydrogen-saturated condition. Measurements were made over a higher temperature range (400–800°K) than was used in the present work. Absolute values of γ were approximately 10 times larger than found in the present work. This is partly attributable to the different technique of measurement, but also to the different physical condition and annealing treatment of the alloys. Eley and Rossington (*15*) found that for the para-H_2 conversion on Au, Ag, and Cu, the activities fell in the order, wires > evaporated films > foils, but that the activation energy was approximately the same for a particular metal in its various physical states. At the lowest temperature of measurement, 400°K, Wood and Wise obtained values of γ as follows: Pd, 0.08; 26.5% Au, 0.12; 44% Au, 0.08; 62% Au, 0.08; Au, 0.13. Extrapolation of these values to room temperature, with the use of their measured activation energies, leads to the following values of γ: Pd, 0.08; 26.5% Au, 0.08; 44.5% Au, 0.05; 62% Au, 0.08; Au, 0.08. That is, at room temperature there is no marked change in γ with composition. It is perhaps significant, though, that the highest activation energy, 1 kcal/mole, was found for Au. These results are broadly in agreement with those of the present work for the *hydrogen-saturated* alloys, except that a relatively higher value of γ for Au was found by Wood and Wise.

Interpretation

The mechanistic consequences of the observed over-all kinetics of atom recombination have been discussed by Ehrlich (*16*). Two routes are available for the recombination of atoms on a surface:

(1) Recombination via a direct encounter of a gas-phase atom and an adsorbed atom. The rate of this process is $Z_1\theta k_d$, where Z_1 is the atomic flux, θ is the fraction of the surface covered with atoms, and k_d is the probability of a successful encounter.

(2) Recombination via the migration of adsorbed atoms over the surface leading to desorption of molecules at a rate $k_m\theta^2$, where k_m has the form $be^{-V/kT}$, and V is the activation energy for desorption.

It is shown in the Appendix that, if the rate of evaporation of atoms, $k_E\theta$, is small, as is certainly the case for hydrogen on metals at room temperature, then in the steady state

$$\gamma = Z_1[1 - \theta(1 - k_d)]/Z_1$$

This relation is quite general and applies irrespective of the mechanism of recombination. It is also valid when a mixture of atoms and molecules is present in the gas phase.

Two situations must now be distinguished:

(a) The molecular gas is not chemisorbed, that is $2D(\text{M–H}) - D(\text{H–H}) < 0$ (a criterion strictly valid only at 0°K). In this case $V \sim V_m$, where V_m is the activation energy for migration (this might be of the order of $\frac{1}{5}D(\text{M–H})$ (*16*).

(b) The molecular gas is chemisorbed, that is $2D(\text{M–H}) - D(\text{H–H}) > 0$. In this case $V = 2D(\text{M–H}) - D(\text{H–H})$ for non-activated chemisorption.

In case (a) the surface coverage in the steady state is determined completely by the relative values of k_m, k_d, and Z_1. It is shown in the Appendix that if $k_m/Z_1 \gg 1$, $\theta \rightarrow 0$, and $\gamma \rightarrow 1$. In this case the rate of adsorption of atoms is the slow, rate-determining, step and the process of atom removal from the gas phase is first order (γ independent of Z_1).

However, if $k_m/Z_1 \ll 1$, and k_d is negligible, as is shown in the Appendix θ is a function of Z_1, and the rate of atom removal becomes kinetically of a lower order than the first. That is, under conditions in which surface migration is important, first order kinetics are *only* found when $\theta \rightarrow 0$ and $\gamma \rightarrow 1$. Hence low values of γ and first order kinetics are incompatible with a migratory mechanism of recombination. On the other hand if k_m is negligible and surface migration cannot take place to any appreciable extent then $\theta = 1/(1 + k_d)$ and $\gamma = 2k_d/(1 + k_d)$. That is, when the direct encounter mechanism is dominant γ is dependent only on k_d and first order kinetics result for all values of γ from 0 to 1.

In case (b) the migratory recombination process cannot by itself determine θ. For strongly chemisorbed species, the equilibrium coverage in the absence of atoms in the gas phase, $\bar{\theta}$, tends to unity, even at room temperature and low pressures. The surface coverage θ, in the presence of both molecules and atoms of the same gas (not in equilibrium), is determined by the rate of dissociative chemisorption Z_2k_a (where Z_2 is the molecular flux), Z_1k_d and the equilibrium coverage $\bar{\theta}$, only; k_m can now be regarded as a dependent variable, related to

$\bar{\theta}$ and Z_2k_a, through $k_m\bar{\theta}^2 = Z_2k_a(1 - \bar{\theta})^2$ (Appendix), and as such k_m cannot control the over-all recombination process. When $\bar{\theta} \rightarrow 1$, i.e. for strong chemisorption, $\gamma \rightarrow 2k_d/(1 + k_d)$ and first order kinetics will again result.

In the present work first order kinetics were found associated with low values of γ, both for Pd on which molecular H_2 is chemisorbed, and on Au on which molecular H_2 is not chemisorbed. It is concluded that in both cases the principal recombination mechanism is via direct encounters, and γ is thus a measure of the probability for the process $M - H + H \rightarrow M + H_2$.

Variation of γ with Composition

The recombination coefficient γ can be expressed in the form $\gamma_0 \exp [-E_d/kT]$, at least for small values of γ. Variation in γ with composition can arise from variation in γ_0, E_d, or both. Although compensation effects are fairly common in catalytic reactions, it is possible, by analogy with the para-H_2 conversion on Pd–Au alloys, that the major change in γ in passing from 50% Au to pure Au is due to an increase in activation energy for the process $M - H + H \rightarrow M + H_2$. The bond energy for Pd–H is 65 kcal/mole (*16*). The corresponding bond energy for Au–H is not known. Since H_2 does not chemisorb on Au, D(Au–H) must presumably be $\leqslant 53$ kcal/mole. Application of Eley's rule (*17*), indicates that it is unlikely to be much less than this value. The increase in activation energy on passing from Pd to Au certainly cannot be related to an increased M–H bond strength. The language of Pauling's theory of metals is useful in discussing this phenomenon. The view can be taken (*18*), that in the formation of a chemisorptive bond with hydrogen a metal employs essentially the same orbitals as used in the formation of metal–metal bonds in the bulk metal, that is (*dsp*) hybrids for Pd, (*sp*) hybrids for Au. In pure Pd, the surface atoms forming Pd–H bonds still possess partly vacant atomic *d* orbitals (~0.6 per atom). Au atoms have no such vacant atomic *d* orbitals. The role of vacant atomic orbitals in promoting catalysis becomes plausible when attention is focused on possible transition states. The vacant *d* orbitals may act as electron acceptors and be utilized in stabilizing a transition complex, possibly of the type

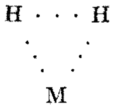

On alloying the Pd with Au the vacant atomic *d* orbitals are filled up and the activation energy increases, the decrease in H–H bond strength failing to compensate for the loss of stabilization energy.

The poisoning effect of hydrogen can then be interpreted [as was done by Couper and Eley (*2*)] by supposing that the sorbed H atoms play a role analogous to that of the Au atoms, namely the donation of electrons to the vacant *d* orbitals of the Pd. The decrease in magnetic susceptibility found experimentally on the sorption of hydrogen by bulk metal (*1*) supports this supposition.

An alternative interpretation of the decrease in catalytic activity on passing from Pd to Au is that vacant atomic *d* orbitals are necessary for the formation of M–H bonds and Au is thus a relatively poor catalyst because it is unable to form Au–H bonds at all. This view is not tenable since in the presence of H atoms, Au does chemisorb hydrogen readily, as the surface potential measurements of Pritchard and Tompkins demonstrate (*19*).

The simple electronic interpretation suggested here broadly satisfies the experimental facts. More elaborate theories would be required to account for the maximum in activity at 30% Au (if genuine) and for the relatively high activity found for the 72% Au alloy. Due to the complexities introduced into this apparently simple system by the solution of hydrogen, such elaboration is unlikely to be profitable at this stage.

Oxygen Atom Recombination

No other studies of oxygen atom recombination on Pd–Au alloys have been reported. The empirical conclusions of the present work are that the recombination process was first order, and that no significant variation in activity with composition was found. Extremely low values of γ were found on the annealed foils; (10^{-3}–10^{-4}).

The value for Au foil may be compared with that of 5.2×10^{-3} obtained by Linnett and Greaves (*9*) for an evaporated metal film. Again the combination of low values of γ with first order kinetics supports a direct encounter mechanism.

Due to the high electronegativity of oxygen, the presence of vacant *d* orbitals (essentially an electron acceptor function) in the alloy is unlikely to facilitate the formation of a transition complex. In the case of Au, the abnormally high ionization potential of the atom will also mitigate against the formation of a stable transition complex. Because of these factors the lack of any systematic variation in γ with alloy composition for oxygen atom recombination, contrasting strongly as it does with the corresponding H atom recombination behavior, supports the simple electronic interpretation of these processes.

ACKNOWLEDGMENTS

We thank the Mond Nickel Co. for the loan of the metal foils and the office of Aerospace Research of the U.S. Air Force for a grant (AF EOAR 62-6).

One of us (W.P.) thanks the Polish Academy of Science and Professor M. Smialowski for making her visit to England possible, and another (P.G.D) the Pressed Steel Co. for a Fellowship.

APPENDIX

THE KINETICS OF ATOM RECOMBINATION

The simple kinetic treatment of atom recombination given here follows and extends that given by Ehrlich (*16*). We consider a metal surface exposed to a flux of particles from a partially dissociated diatomic gas. The rate of surface coverage is

$$n_s(d\theta/dt) = Z_1(1 - \theta) - Z_1\theta k_d - k_e\theta - 2k_m\theta^2 + 2Z_2k_a(1 - \theta)^2 \quad (1)$$

where

n_s is the number of adsorption sites/unit area;

θ, the fraction of sites occupied;

Z_1, the atomic flux, and Z_2, the molecular flux;

$Z_1\theta k_d$, the rate of successful atom recombination via direct encounters between gas phase atoms and adsorbed atoms ($k_d < 1$);

θk_e, the rate of evaporation of adsorbed atoms ($k_e \propto e^{-\chi/kT}$, where $\chi = D(\text{M–H})$);

$2k_m\theta^2$, the rate of atom recombination via surface migration and molecular desorption;

$Z_2k_a(1 - \theta)^2$, the rate of dissociative chemisorption ($k_a \leqslant 1$).

We use as far as possible the same notation as Ehrlich (*16*). A condensation coefficient of unity for atom adsorption is assumed. At room temperature the rate of evaporation of adsorbed atoms is completely negligible ($\chi \sim 50$ kcal/mole) and the term $k_e\theta$ is neglected. The surface recombination coefficient γ is defined for the steady state, ($d\theta/dt = 0$), by

$$\gamma = \frac{\text{number of atoms arriving/sec} - \text{number of atoms leaving/sec}}{\text{number of atoms arriving/sec}}$$

$$= [Z_1 - Z_1\theta(1 - k_d)]/Z_1$$

$$= 1 - \theta(1 - k_d) \qquad (k_e\theta \text{ neglected}) \quad (2)$$

If only molecular gas is present ($Z_1 = 0$) an equilibrium coverage, $\bar{\theta}$, is obtained where $k_m\bar{\theta}^2 = Z_2k_a(1 - \bar{\theta})^2$; therefore

$$Z_2k_a = k_m\alpha \quad \text{where} \quad \alpha = \bar{\theta}^2/(1 - \bar{\theta})^2$$

$\bar{\theta}$ is determined solely by the free energy change of chemisorption; for strong chemisorption $\bar{\theta} \sim 1$; for no chemisorption, $\bar{\theta} \sim 0$, $\alpha = 0$. Substituting for Z_2k_a in (1) and neglecting $k_e\theta$, we find for the steady state

$$\theta = \frac{[Z_1(1 + k_d) + 4\alpha k_m] - [Z_1{}^2(1 + k_d)^2 + 8\alpha k_m Z_1 k_d + 8k_m Z_1 + 16k_m{}^2\alpha]^{1/2}}{4k_m(\alpha - 1)} \quad (3)$$

Two extreme cases may be considered: (*i*) $\alpha = 0$ (molecular gas *not* chemisorbed); (*ii*) $\alpha \rightarrow \infty$ (molecular gas strongly chemisorbed).

Case (*i*). Two subcases arise:

(a) Suppose $k_d \sim 0$ (direct encounter mechanism negligible); then (see Ehrlich, ref. *16*)

$$\theta = (Z_1/4k_m)/[(1 + 8k_{m/Z_1})^{1/2} - 1]$$

From (2) $\gamma = 1 - \theta$. In Fig. 6, γ is plotted as a function of Z_1/k_m. It is clear that γ is independent of Z_1, and hence of the gas

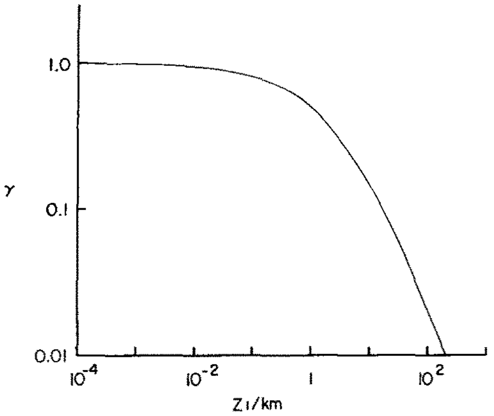

FIG. 6. Variation of γ with Z_1/k_m.

phase atom concentration, only when $\theta \to 0$ and $\gamma \to 1$. When $Z_1/k_m \gg 1$, $\theta \to 1$, $\gamma \to 0$, and γ becomes inversely proportional to Z_1. That is, the rate of disappearance of atoms from the gas phase, which is proportional to $Z_1\gamma$ is first order in atom concentration only when $\gamma \to 1$ and $\theta \to 0$. Small values of γ are incompatible with first order kinetics when a migratory recombination mechanism is dominant.

(b) Suppose $k_m/Z_1 \ll 1$ (migratory recombination mechanism negligible) but k_d finite (direct encounter mechanism operative). Then,

$$\theta \to 1/(1 + k_d) \quad \text{and} \quad \gamma \to 2k_d/(1 + k_d)$$

γ is independent of Z_1 and hence first order kinetics result for all values of γ.

Case (ii). We transform θ into $f(Z_2)$ by writing $\alpha k_m = k_a Z_2$ in Eq. (3). Let $Z_1/Z_2 = \beta$, whence,

$$\theta = \frac{Z_2[\beta(1 + k_d) + 4k_a] - Z_2[(1 + k_d)^2\beta^2 + 8\beta k_a k_d + 8\beta k_a/\alpha + 16k_a/\alpha^2]^{1/2}}{4Z_2 k_a(\alpha - 1)/\alpha} \tag{4}$$

For strong, nonactivated molecular chemisorption $\alpha \to \infty$ and $k_a = 1$. Whence,

$$\theta = \tfrac{1}{4}\{[\beta(1 + k_d) + 4] - (1 + k_d)\beta[1 + 8k_d/(1 + k_d)^2\beta]^{1/2}\}$$

Hence under these conditions γ is unaffected by k_m and its value is determined solely by the direct encounter mechanism. Typically, β is about 0.1 (~10% atoms in the gas mixture). If k_d is small such that, $8k_d/(1 + k_d)^2 \ll 1$, then $\theta \to 1/(1 + k_d)$, and $\gamma \to 2k_d/(1 + k_d)$ as in case (*i*b) above. Typical values for $\beta = 0.1$ are shown below.

$k_d = 0.01$ $\theta = 0.0186$
$k_d = 0.1$ $\theta = 0.129$
$k_d = 0.5$ $\theta = 0.56$
$k_d = 1$ $\theta = 1$

REFERENCES

1. VOGT, E., *Ann. Physik.* **14,** 1 (1932).
2. COUPER, A., AND ELEY, D. D., *Discussions Faraday Soc.* **8,** 172 (1950).
3. RIENÄCKER, G., AND SARRY, B., *Z. Anorg. Allgem. Chem.* **257,** 41 (1948).
4. RIENÄCKER, G., AND VORMUM, G., *Z. Anorg. Allgem. Chem.* **283,** 287 (1948).
5. BOND, G. C., "Catalysis by Metals." Academic Press, London, 1962.
6. SMITH, W. V., *J. Chem. Phys.* **11,** 110 (1943).
7. DICKENS, P. G., SCHOFIELD, D., AND WALSH, J., *Trans. Faraday Soc.* **56,** 225 (1960).
8. SCHOFIELD, D., D.Phil. Thesis, Oxford, 1960.
9. GREAVES, J. C., AND LINNETT, J. W., *Trans. Faraday Soc.* **54,** 1324 (1958).
10. KAUFMANN, F., AND DEL GRECO, F. P., *Symp. Combust. 9th 1963,* p. 659.
11. AMDUR, I., *J. Chem. Phys.* **4,** 339 (1936).
12. ANDRUSSOV, L., *Z. Electrochem.* **54,** 566 (1950); **55,** 51 (1951).
13. SMITH, D. P., "Hydrogen in Metals." Univ. of Chicago Press, 1948.
14. WOOD, B., AND WISE, H., *J. Phys. Chem.* **65,** 1976 (1961).
15. ELLEY, D. D., AND ROSSINGTON, D. R., *in* "Chemisorption." Butterworths, London, 1957.
16. EHRLICH, G., *J. Chem. Phys.* **31,** 1111 (1959).
17. ELEY, D. D., *Discussions Faraday Soc.* **8,** 34 (1950).
18. DOWDEN, D. A., *in* "Chemisorption." Butterworths, London, 1957.
19. PRITCHARD, J., AND TOMPKINS, F. C., *Trans. Faraday Soc.* **56,** 540 (1960).